UDC 620.22:546.05

DOI: 10.15372/KhUR20170112

Catalytic Synthesis and Studies of Nitrogen Doped Multiwall Carbon Nanotubes

A. N. SUBOCH[1,2], L. S. KIBIS[1,2], O. A. STONKUS[1,2], D. A. SVINTSITSKIY[1,2], A. B. AYUSHEEV[1], Z. R. ISMAGILOV[1,3], and O. YU. POD'YACHEVA[1,2]

[1]*Boreskov Institute of Catalysis, Siberian Branch, Russian Academy of Sciences, Novosibirsk, Russia*

E-mail: arina@catalysis.ru

[2]*Novosibirsk National Research State University, Novosibirsk, Russia*

[3]*Institute of Coal Chemistry and Material Science, Siberian Branch, Russian Academy of Sciences, Kemerovo, Russia*

Abstract

Homogeneous nitrogen-doped bamboo-like carbon nanotubes (N-CNTs) with the carbon content up to 7.3 at. % were obtained by catalytic decomposition of ordinary ethylene/ammonia mixture. Physicochemical properties of N-CNTs were studied by X-ray analysis, X-ray photoelectron spectroscopy, transmission electron microscopy and Raman spectroscopy methods. The effect of the synthesis temperature, catalyst nature and reaction mixture composition per the amount of nitrogen, ratio of its forms, defectiveness and morphology of N-CNTs was determined.

Key words: carbon nanotubes, nitrogen doping, catalytic decomposition, ethylene, ammonia

INTRODUCTION

Carbon nanomaterials (CNMs) due to their unique physicochemical properties can be used in composites for nanoelectronics and sensors, as well as catalysts and adsorbents carriers. Special attention is paid to two types of CNMs: carbon nanotubes (CNTs) and carbon nanofibres (CNFs) with various ways of packaging graphite layers due to the simplicity of their preparation. Works on the elaboration of the chemical modification of CNTs and CNF for the preparation of new materials for various applications have been carried out in the last decades [1]. One of the possible modification methods of carbon nanomaterials is their doping with heteroatoms, for example, with nitrogen [2]. Thus, the introduction of nitrogen into CNFs leads to stabilizing subnanometer applied platinum particles [3] or to changing the electron condition of cobalt in Co-containing composites based on N-CNF [4], which contributes to improving catalytic properties of new materials in various processes. It is known that nitrogen in CNM is found in three major states: pyridine-like, pyrrole and graphite-like (three-coordinated) [2]. Herewith, due to its structural peculiarities, the most accessible centre in N-CNF for the interaction with applied components is pyridine-like nitrogen, and in N-CNTs, all nitrogen forms are equally accessible. For this reason, N-CNTs are of large interest for applying as catalyst carrier.

There are two major approaches to the preparation of N-CNTs to date: 1) direct synthesis from a nitrogen-containing precursor or a mixture of nitrogen- and carbon-containing compounds [5–10] and 2) post-treatment of carbon

© Suboch A. N., Kibis L. S., Stonkus O. A., Svintsitskiy D. A., Ayusheev A. B., Ismagilov Z. R., and Pod'yacheva O. Yu., 2017

materials in a nitrogen-containing atmosphere [20, 21]. Among direct synthesis methods, chemical vapour deposition is simplest in implementation and allows most precisely regulating properties of obtainable products. As a carbon source, methane [7, 10, 12], acetylene [6, 8–10, 13] or ethane [5, 12] are used, and as a nitrogen source – ammonia [5–13], pyridine [15, 16, 19], acetonitrile [17–19], dimethylformamide [14] *etc*. As a rule, catalysts based on Fe [6, 7, 10–12, 14, 15, 19] are used in the synthesis process of N-CNT from hydrocarbons, and nitrogen content reaches 5 at. %. N-CNTs with a high yield (10 g C/g catalyst), and nitrogen content up to 7.4 at. % were obtained only in work [19].

Other transition metals are also used for the synthesis of N-CNTs. For example, in case of the use of a Co–Mg–MoO_4 catalyst, high yields of N-CNT (30 g C/g catalyst) were observed; however, nitrogen content amounted to no more than 3 at. % [12]. Works on the synthesis of N-CNT on MgO [7] or Ni/Si [8] catalysts are also found in the literature. It is noteworthy that the use of complex organic compounds does not allow reaching high yields of N-CNTs and nitrogen content [14–16]. Additionally, the application of organic precursors requires complex instrumentation for conducting the process. Due to this, the preparation problem of N-CNTs with controllable properties from simple and inexpensive precursors is quite relevant.

The purpose of this work is the elaboration of the method of synthesis of N-CNTs by decomposition of ethylene-ammonia mixture and study of the effect of conditions of conducting the process and catalyst type on physicochemical properties of N-CNTs.

EXPERIMENTAL

Synthesis of catalysts

Catalysts with the composition of 90 % Fe–10 % Al_2O_3 (90Fe–Al_2O_3), 62 % Fe–8 % Ni–30 % Al_2O_3 (62Fe–8Ni–Al_2O_3) and 85 % Fe–5 % Co–10 % Al_2O_3 (85Fe–5Co–Al_2O_3) were prepared by the co-precipitation method from water solutions of nitrates followed by calcination of precipitates in air at 450 °C. Calcined samples were reduced in an atmosphere of hydrogen at 550–580 °C in a flow reactor with the vibrofluidized catalyst layer at a pressure of 1 bar. After reduction, the catalyst was cooled in a flow of H_2, passivated with ethanol *in situ* and dried in air at room temperature during 24–28 h.

Synthesis of N-CNTs

Nitrogen-doped carbon nanotubes were synthesized by decomposition of ethylene/ammonia mixture on the resulting catalysts in a flow reactor at 600–700 °C. The concentration of ammonia in the initial mixture was varied from 25 to 75 vol. %. The catalyst loading was 0.1 g, and a flow of the reaction mixture – 22.5 L/(g_{cat} · h). To remove adsorbed oxygen from the catalyst surface its preliminary reduction in situ during 15 min at synthesis temperature. The gas mixture composition at the reactor exit was measured by chromatographic analysis. The reaction was carried out until catalyst deactivation. Upon completion of the process, the reactor was cooled in a flow of argon.

Carbon nanotubes not containing nitrogen (MWCNT) were obtained using a 62Fe–8Ni–Al_2O_3 catalyst by decomposition of ethylene at 700 °C and a pressure of 1 bar.

Physicochemical research methods

X-ray phase analysis (XPA) spectra were recorded using a Bruker D8 Advance (Germany) diffractometer with CuK_α radiation. Data recording was conducted in the areas of 2θ angles from 5 to 80° with a step of 0.05° and acquisition time of 5 s at each point.

X-ray photoelectron spectroscopy (XPS) spectra were obtained using a KRATOS ES300 photoelectron spectrometer. A source of AlK_α radiation without a monochromator ($h\nu$ = 1486.6 eV) was used for surveying spectra of internal levels of gold Au4$f_{7/2}$ and copper Cu2$p_{3/2}$with bond energies equal to 84.0 and 932.7 eV, respectively, were used for calibrating the energy scale.

Quantitative control of the surface chemical composition was performed according to survey spectra recorded in a range of

0–1100 eV with an energy resolution corresponding to the maximum sensibility of the transmittance energy of the spectrometer, HV = 50 eV and scan step of 1 eV. To analyze the chemical composition and charge states of carbon and nitrogen recording the narrow regions of C1*s* and N1*s* with HV = 25 eV and scan step of 0.1 eV was carried out.

Processing of the resulting experimental data was carried out in the XPSCalc program that was widely used by us earlier for analysis of carbon-containing systems [23, 24]. Background subtraction was carried out using the Shirley method. Decomposition of experimental spectra of nitrogen into individual components was carried out using a combination of Gaussian and Lorentz functions.

The morphology of the tubes obtained was studied by transmission electron microscopy (TEM) using a JEM-2200FS microscope (JEOL Ltd., Japan) with an accelerating voltage of 200 kV and the lattice spatial resolution of 1 Å.

Raman scattering (RS) spectra were removed using a HORIBA LabRAM HR800 instrument equipped with a laser with a wavelength of 632.8 nm and diffraction grating of 1800 g/mm. Laser pumping at the entrance was 0.7 mV. A 50X LWD objective ensured the laser spot size of 1.4 μm. Measurements for each sample were carried out in a range from 65 to 3800 cm^{-1}. Herewith, the final spectrum was obtained by summing up individual measurements with an exposure of 120 s and five-fold accumulation cycle. Decomposition of spectra into components was performed using a combination of the Gaussian and Lorentz functions with the Lorentzian component of over 0.85.

TABLE 1

Synthesis conditions of N-CNTs, carbon intensity and nitrogen content in N-CNTs

Synthesis conditions			Carbon	[N],
Catalysts	NH_3 content in mixture, %	*T*, °C	intensity, g C/g_{cat}	at. %
$90Fe–Al_2O_3$	60	700	1.5	
$62Fe–8Ni–Al_2O_3$	0	700	38	–
	25	650	7	2.8
		700	30	1.7
	40	700	22	3.1
	60	600	0.5	9.8
		650	5	6.7
		700	12	5.2
	75	650	6	7.3
		700	10	5.0
$85Fe–5Co–Al_2O_3$	60	650	1	2.8
		700	2	1.7
$75Co–Al_2O_3$	60	550	12	3.0
		600	13	2.6
		650	10	1.5

RESULTS AND DISCUSSION

To determine optimum conditions of the synthesis of N-CNTs by the catalytic decomposition method we conducted a systematic study of the effect of various synthesis parameters on physicochemical properties of the obtainable materials: temperature, the ammonia content in the reaction mixture (Table 1).

Earlier, it was demonstrated in works [5, 9–11, 19] that Fe- and Co-containing catalysts were some of most promising for the synthesis of N-CNTs, since they allow obtaining significant yields of the material and relatively high nitrogen content in CNTs. Additionally, it was demonstrated that the addition of the second Co or Ni metal in amounts up to 10 mass % leads to a significant increase in the catalyst stability [22]. That is why the following catalysts were used for the synthesis of N-CNT: $90Fe–Al_2O_3$, $62Fe–8Ni–Al_2O_3$, $85Fe–5Co–Al_2O_3$, $75Co–Al_2O_3$.

Comparative analysis of catalysts allowed determining that an active yield growth of CNMs was observed in case of the use of $62Fe–8Ni–Al_2O_3$ and $75Co–Al_2O_3$ catalysts, the product yield reached 30 g C/g catalyst. In its turn, the yield of N-CNMs on $85Fe–5Co–Al_2O_3$ and $90Fe–Al_2O_3$ catalysts did not exceed 2 g C/g catalyst. When comparing the amount of nitrogen in the material depending on the catalyst nature and synthesis temperature it was demonstrated that when using a 40 % C_2H_4/ 60 % NH_3 mixture the largest amount of nitrogen is observed in the material obtained on a $62Fe–8Ni–Al_2O_3$ catalyst at 600 °C. However, it was demonstrated by TEM that the material represented the carbonized catalyst particles. It was determined by the same method that in

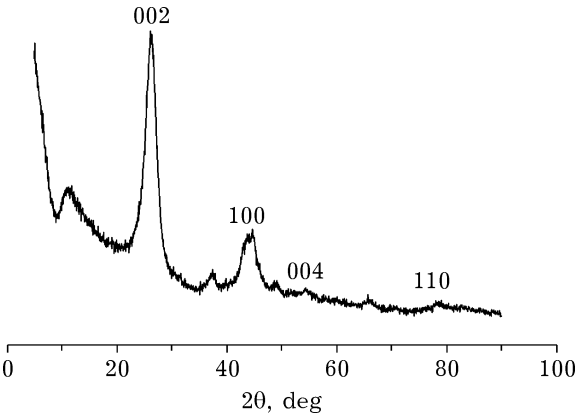

Fig. 1. XPA spectrum of N-CNTs synthesized at 650 °C by decomposition of a 40 % C_2H_4/60 % NH_3 mixture over a 62Fe–8Ni–Al_2O_3 catalyst.

case of using the Co-based catalyst N-CNT with coaxially conical packing of graphite layers were formed, and in case of a Fe-based catalyst – homogeneous, bamboo-like nanotubes representing multiwall carbon nanotubes with regular interior partitions. Based on the data obtained about the morphology and yield of Na-CNT a 62Fe–8Ni–Al_2O_3 bimetallic catalyst was selected for further studies.

A study was carried out on the effects of the ammonia content in the reaction mixture on properties of N-CNTs. It was determined that an increase in the ammonia content in the mixture leads to a decrease in the yield of N-CNT from 30 to 5 g C/g catalyst, however, the

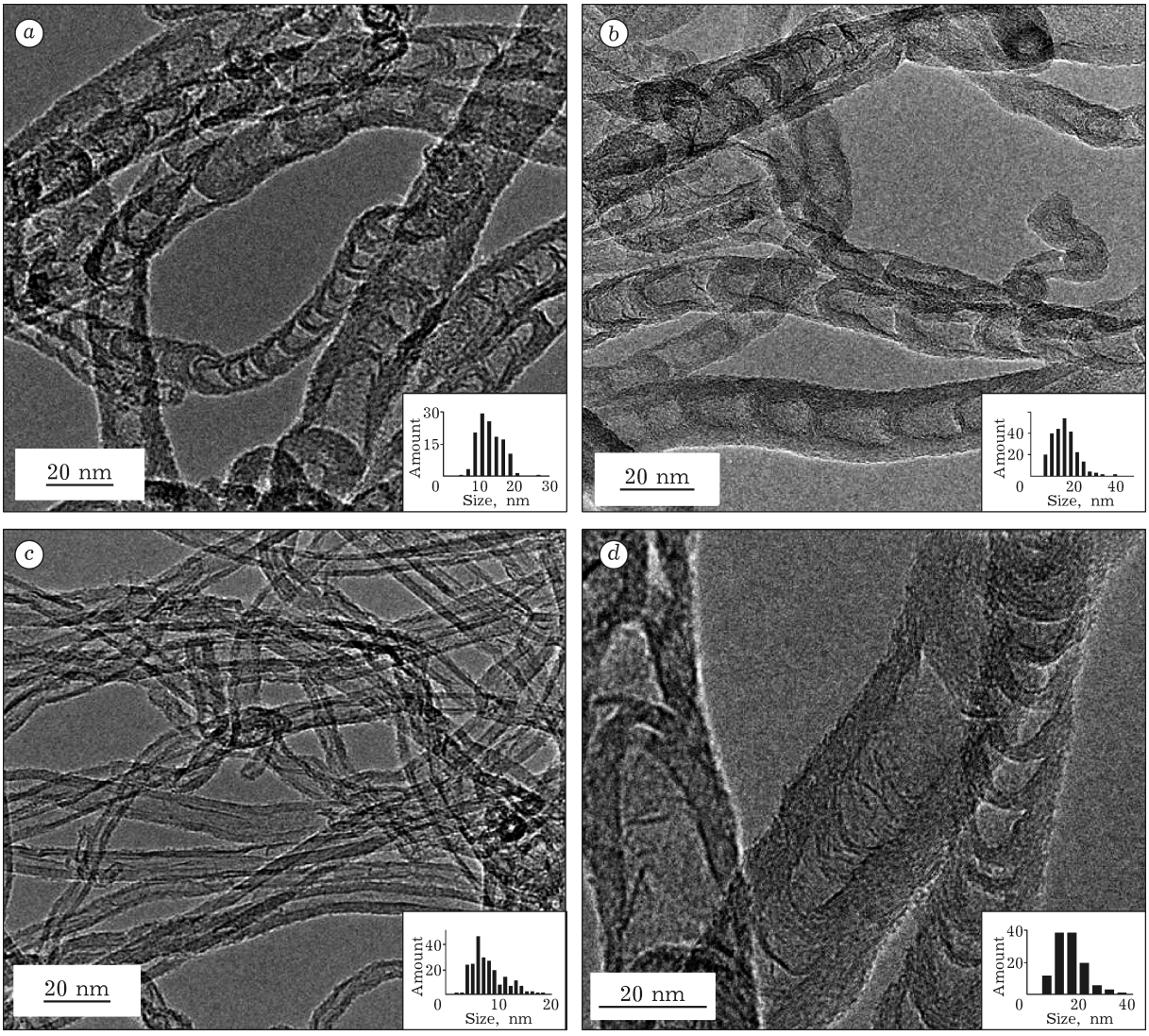

Fig. 2. TEM images of N-CNTs synthesized over a 62Fe–8Ni–Al_2O_3 catalyst by decomposition of a 40 % C_2H_4/60 % NH_3 mixture: *a* and *b* – at 650 and 700 °C, respectively; *c* – MWCNTs; *d* – N-CNTs obtained by decomposition of a 25 % C_2H_4/75 % NH_3 mixture at 650 °C.

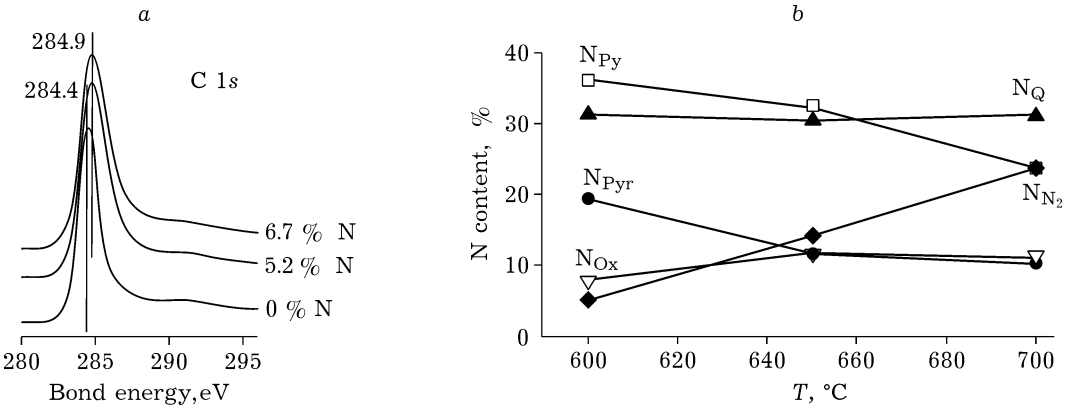

Fig. 3. XPS spectra of C1*s* MWCNTs and N-CNTs (*a*) and ratio of nitrogen forms in N-CNTs obtained over a 62Fe–8Ni–Al_2O_3 catalyst by decomposition of a 40 % C_2H_4/60 % NH_3 mixture *vs* the synthesis temperature (*b*). N_{Py} – pyridine-like nitrogen, N_Q – graphite-like nitrogen, N_{Pyr} – pyrrole nitrogen, N_{Ox} – oxidized nitrogen, N_{N_2} – molecular nitrogen.

content of nitrogen herewith increased from 1.7 to 7.3 at. %. It should be noted that, according to the literature data, only in case of decomposition of complex organic compounds, such as acetonitrile or pyridine, yields of N-CNT comparable by the content of nitrogen were observed [18].

The study of samples by the XPA method demonstrated that all the materials obtained were graphite like with an interplanar spacing d_{002} ~ 3.4 Å. As an example, the spectrum of N-CNTs obtained on a catalyst by decomposition of the 40 % C_2H_4/60 % NH_3 mixture at 650 °C is presented in Fig. 1.

The TEM method demonstrated that the synthesized N-CNTs represented homogeneous bamboo-like tubes with a diameter of 13–16 nm and a length of 1–2 mm, unlike MWCNT, an average diameter of which is 8 nm (Fig. 2). An active increase in of CNT is observed at temperatures above 650 °C. An increase in the synthesis temperature is accompanied by an increase in the length of tubes from 5 to 10 μm, diameter – from 13 to 16 nm, and a length of segments – from 10 to 25 nm. In its turn, an increase in ammonia proportion in the reaction mixture also leads to a change in the morphology of tubes: forming a more pronounced bamboo- like structure is observed and the length of segments decreases approximately in three times. Segments of CNTs consist on average 5–10 of graphene layers; moreover, the thickness of partitions does not differ from the wall thickness of tubes.

It was demonstrated by XPS studies that C1*s* spectra of the resulting MWCNTs and N-CNTs had the structure typical for CNTs. The position of the maximum peak in a region of 284.4–284.9 eV and density availability in an area of 290–292 eV indicate a sp^2 hybridized carbon structure (Fig. 3, *a*). A slight shift of the maximum of the C1*s* spectrum to the side of larger bond energies and peak broadening observed for nitrogen-containing N-CNT samples speak of nitrogen introducing into the structure of nanotubes [25]. According to XPS data, the amount of nitrogen in N-CNTs is varied from 1.7 to 7.3 at. %. An increase in the reaction temperature is accompanied by a decrease in the nitrogen content, and an increase in the ammonia content on the contrary leads to an increase in nitrogen concentration in N-CNTs. Nitrogen in N-CNTs is found in the pyridine-like (~398.5 eV), pyrrole (~399.5 eV), graphite-like (~401.0 eV), oxidized (~402.5 eV) and molecular (~405 eV) [25, 26] states. The ratio of nitrogen forms is changed with an increase in temperature: the proportion of the pyridine and pyrrole nitrogen is decreased and the proportion of the capsulated N_2 increases (see Fig. 3, *b*). Different stabilities of nitrogen forms explain this [27].

The peaks at ~1350 cm^{-1} (*D* line), ~1580 cm^{-1} (*G* line), 1620 cm^{-1} (*D′* line) and 2700 cm^{-1} (*G′* line) are registered in Raman spectra of MWCNTs and N-CNTs [28]. Nitrogen-doping of MWCNTs is accompanied by the shift of the maxima to the region of large frequencies and

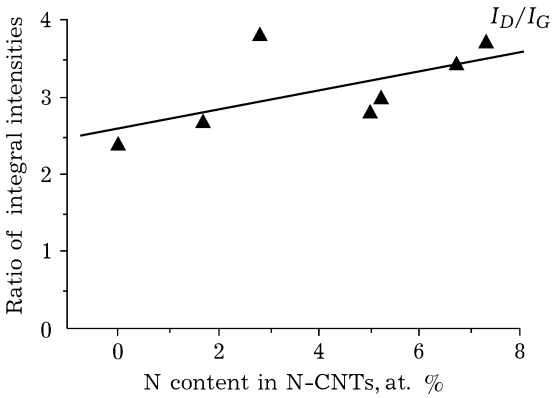

Fig. 4. Ratio of I_D/I_G intensities *vs* the total nitrogen content in N-CNTs obtained over a 62Fe–8Ni–Al_2O_3 catalyst.

by a monotonic increase of the I_D/I_G ratio from 2.4 to 3.8, which testifies an increase in the defectiveness of the N-CNT structure in comparison with MWCNTs (Fig. 4). These results correlate with the data obtained earlier for N-CNFs, where an analogous monotonic increase in the I_D/I_G ratio with an increase in nitrogen content in carbon nanofibres was demonstrated [29].

CONCLUSION

Thus, systematic analysis of various composition catalysts demonstrated that the use of the 62Fe–8Ni–Al_2O_3 catalyst allowed obtaining homogeneous bamboo-like C-NTs with nitrogen content up to 7.3 at. % and the yield up to 30 g C/g catalyst using catalytic decomposition of ordinary ethylene-ammonia mixture. It was demonstrated that the nitrogen content, its forms ratio, as well as the morphology and defectiveness of N-CNTs was changed depending on the synthesis temperature, ammonia concentration in the reaction mixture, and consequently, by selecting certain process conditions one can obtain N-CNTs with specified properties.

REFERENCES

1 Filho A. G. S., Terrones M., *B-C-N Nanotubes and Related Nanostructures*, 6 (2009) 223.
2 Ciric-Marjanovic G., Pasti I., Mentus S., *Prog. Mater. Sci.*, 69 (2014) 61.
3 Jia L., Bulushev D. A., Podyacheva O. Yu., Boronin A. I., Kibis L. S., Gerasimov E. Y., Beloshapkin S., Seryak I. A., Ismagilov Z. R., Ross J. R. H., *J. Catal*, 307 (2013) 94.
4 Podyacheva O. Yu., Stadnichenko A. I., Yashnik S. A., Stonkus O. A., Slavinskaya E. M., Boronin A. I., Puzynin A. V., Ismagilov Z. R., *Chin. J. Cat.*, 35, 6 (2014) 960.
5 Chizari K., Janowska I., Houlle M., Florea I., Ersen O., Romero T., Bernhardt P., Ledoux M. J., Pham-Huu C., *Appl. Catal. A*, 380 (2010) 72.
6 Lee C. J., Lyu S. C., Kim H. W., Lee J. H., Cho K. I., *Chem. Phys. Lett.*, 359 (2002) 115.
7 Ning G., Xu C., Zhu X., Zhang R., Qian W., Wei F., Fan Z., Gao J., *Carbon*, 56 (2013) 38.
8 Kim T. Y., Lee K. R., Eun K. Y., Oh K. H., *Chem. Phys. Lett.*, 372 (2003) 603.
9 Jang J. W., Lee C. E., Lyu S. C., Lee T. J., Lee C., *J. Appl. Phys. Lett.*, 84 (2004) 2877.
10 Lee Y. T., Kim N. S., Bae S. Y., Park J., Yu S. C., Ryu H., Lee H. J., *J. Phys. Chem. B.*, 107 (2003) 12958.
11 Doung-Viet C., Ba H., Liu Yu., Truong-Phuoc L., Nhut J.-M., Pham-Huu C., *Chin. J. Catal.*, 35 (2014) 906.
12 Tao X. Y., Zhang X. B., Sun F. Y., Cheng J. P., Liu F., Luo Z. Q., *Diamond Relat. Mater.*, 16 (2007) 425.
13 García-García F. R., Álvarez-Rodríguez J., Rodríguez-Ramos I., Guerrero-Ruiz A., *Carbon*, 48 (2010) 267.
14 Tang Ch., Bando Y., Golberg D., Xu F., *Carbon*, 42 (2004) 2625.
15 Sadek A. Z., Zhang C., Hu Z., Partridge J. G., McCulloch D. G., Wlodarski W., and Kalantar-Zadeh K., *J. Phys. Chem. C*, 114 (2010) 238.
16 Jian G., Zhao Y., Wu Q., Yang L., Wang X., Hu Z., *J. Phys. Chem. C*, 117 (2013) 7811.
17 Xue R., Sun Z., Su L., Zhang X., *Catal. Lett.*, 135 (2010) 312.
18 Mamo M. A, Sustaita A. O., Tetana Z. N., Coville N. J., Hümmelgen I. A., *J. Mater. Sci.*, 24, 10 (2013) 3995.
19 Dommele S. van, Romero-Izquirdo A., Brydson R., Jong K. P. de, Bitter J. H., *Carbon.*, 46 (2008) 138.
20 Arrigo R., Havecker M., Wrabetz S., Blume R., Lerch M., McGregor J., Parrott E. P. J., Zeitler J. A., Gladden L. F., Knop-Gericke A., Schlögl R., Su D. S., *J. Am. Chem. Soc.*, 132 (2010) 9616.
21 Basiuk E. V., Monroy-Pel'az M., Puente-Lee I, Basiuk V., *Nano Lett.*, 4, 5 (2004) 863.
22 Reshetenko T. V., Avdeeva L. B., Khassina A. A., Kustova G. N., Ushakov V. A., Moroz E. M., Shmakov A. N., Kriventsov V. V., Kochubey D. I., Pavlyukhin Yu. T., Chuvilin A. L., Ismagilov Z. R., *Appl. Catal. A: Gen.*, 168 (2004) 127.
23 Podyacheva O. Yu., Ismagilov Z. R., Boronin A. I., Kibis L. S., Slavinskaya E. M., Noskov A. S., Shikina N. V., Ushakov V. A., Ischenko A. V., *Catal. Today*, 186, 1 (2012) 42.
24 Zacharska M., Podyacheva O. Yu., Kibis L. S., Boronin A. I., Senkovskiy B. V., Gerasimov E. Y., Taran O. P., Ayusheev A. B., Parmon V. N., Leahy J. J., Bulushev D. A., *Chem. Catal. Chem.*, 7, 18 (2015) 2910.
25 Susi T., Pichler T., Ayala P., *J. Nanotechnol.*, 6, 1 (2015) 177.
26 Bulusheva L. G., Okotrub A. V., Fedoseeva Y. V., Kurenya A. G., Asanov I. P., Vilkov O. Y., Koys A. A., Grobert N., *Phys. Chem. Chem. Phys.*, 14, 37 (2015) 237417.
27 Fujisawa K., Tojo T., Muramatsu H., Elias A. L., Vega-Diaz S. M., Tristan-Lopez F., Kim J. H., Hayashi T., Kim Y. A., Endo M., Terrones M., *Nanoscale*, 3 (2011) 4359.
28 Dresselhaus M. S., Dresselhaus G., Saito R., Jorio A., *Phys. Rep.*, 409, 2 (2005) 47.
29 Ismagilov Z. R., Shalagina A. E., Podyacheva O. Yu., Ischenko A. V., Kibis L. S., Boronin A. I., Chesalov Yu. A., Kochubey D. I., Romanenko A. I., Anikeeva O. B., Buryakov T. I., Tkachev E. N., *Carbon*, 47 (2009) 1922.